ESC
European Society
of Cardiology

Genetic deletion of p66shc and/or cyclophilin D results in decreased pulmonary vascular tone

Mareike Gierhardt[1,2,3,†]Oleg Pak[1], Akylbek Sydykov [1], Simone Kraut[1], Julia Schäffer[1],
Claudia Garcia[1], Christine Veith[1], Esraa M. Zeidan[1,4], Monika Brosien[1], Karin Quanz[1],
Azadeh Esfandiary[1], Alireza Saraji [1], Stefan Hadzic [1], Baktybek Kojonazarov[1,5],
Jochen Wilhelm[1,5], Hossein A. Ghofrani[1,6], Ralph T. Schermuly[1], Werner Seeger[1,3],
Friedrich Grimminger[1], Christiane Herden[7], Rainer Schulz[8],
Norbert Weissmann [1]*, Jacqueline Heger[8§] and Natascha Sommer [1§]

[1]Excellence Cluster Cardio Pulmonary Institute (CPI), University of Giessen and Marburg Lung Center (UGMLC), Member of the German Center for Lung Research (DZL), Justus-Liebig University, Giessen, Germany; [2]Instituto de Investigación en Biomedicina de Buenos Aires (IBioBA) - CONICET - Partner Institute of the Max Planck Society, Buenos Aires, Argentina; [3]Department of Lung Development and Remodeling, Max Planck Institute for Heart and Lung Research, Member of the German Center for Lung Research (DZL), Member of the Cardio-Pulmonary Institute (CPI), Bad Nauheim, Germany; [4]Department of Pharmacology and Toxicology, Faculty of Pharmacy, Minia University, El-Minia, Egypt; [5]Institute for Lung Health (ILH), Giessen, Germany; [6]Department of Medicine, Imperial College London, Du Cane Road, Hammersmith Campus, London, W12 0NN, UK; [7]Institute of Veterinary Pathology, Justus-Liebig University, Giessen, Germany; [8]Institute of Physiology, Justus-Liebig University, Giessen, Germany

Aims	The pulmonary vascular tone and hypoxia-induced alterations of the pulmonary vasculature may be regulated by the mitochondrial membrane permeability transition pore (mPTP) that controls mitochondrial calcium load and apoptosis. We thus investigated, if the mitochondrial proteins p66shc and cyclophilin D (CypD) that regulate mPTP opening affect the pulmonary vascular tone.
Methods and results	Mice deficient for p66shc (p66shc$^{-/-}$), CypD (CypD$^{-/-}$), or both proteins (p66shc/CypD$^{-/-}$) exhibited decreased pulmonary vascular resistance (PVR) compared to wild-type mice determined in isolated lungs and *in vivo*. In contrast, systemic arterial pressure was only lower in CypD$^{-/-}$ mice. As cardiac function and pulmonary vascular remodelling did not differ between genotypes, we determined alterations of vascular contractility in isolated lungs and calcium handling in pulmonary arterial smooth muscle cells (PASMC) as underlying reason for decreased PVR. Potassium chloride (KCl)-induced pulmonary vasoconstriction and KCl-induced cytosolic calcium increase determined by Fura-2 were attenuated in all gene-deficient mice. In contrast, KCl-induced mitochondrial calcium increase determined by the genetically encoded Mito-Car-GECO and calcium retention capacity were increased only in CypD$^{-/-}$ and p66shc/CypD$^{-/-}$ mitochondria indicating that decreased mPTP opening affected KCl-induced intracellular calcium peaks in these cells. All mouse strains showed a similar pulmonary vascular response to chronic hypoxia, while acute hypoxic pulmonary vasoconstriction was decreased in gene-deficient mice indicating that CypD and p66shc regulate vascular contractility but not remodelling.
Conclusions	We conclude that p66shc specifically regulates the pulmonary vascular tone, while CypD also affects systemic pressure. However, only CypD acts via regulation of mPTP opening and mitochondrial calcium regulation.

*Corresponding author. Tel: +49 641 99 46000; +49 641 99 42422 (assistant); fax: +49 641 99 42419, E-mail: Norbert.Weissmann@innere.med.uni-giessen.de

Graphical Abstract

1. Introduction

Mitochondria play an important role in the regulation of cellular calcium homeostasis. This is accomplished through the mitochondrial matrix uptake and release of calcium and through the release of reactive oxygen species (ROS).[1] Calcium is known to be crucial for the contraction of pulmonary arterial smooth muscle cells (PASMCs).[2] Thus, mitochondria may be involved in regulating pulmonary vascular tone by interfering with PASMC calcium homeostasis. Moreover, mitochondria have been shown to be particularly important for the pulmonary vascular responses to hypoxia, including hypoxic pulmonary vasoconstriction (HPV) and hypoxia-induced pulmonary hypertension (PH).[3]

The contraction of small pulmonary arteries in response to alveolar hypoxia, known as HPV or the von Euler–Liljestrand mechanism, matches local blood perfusion to alveolar ventilation, thereby protecting the organism against life-threatening hypoxaemia.[4,5] Although the exact underlying mechanism of HPV remains unknown, an intracellular increase of calcium in PASMCs is assumed to be sufficient to induce contraction, at least during the very fast acute phase of HPV, which occurs within seconds.[2,3] Sustained HPV (lasting minutes to hours) may additionally rely on other mechanisms, such as calcium sensitization.[6] In addition to HPV, chronic exposure to hypoxia, as occurs at high altitudes or when induced by lung diseases, leads to a dysregulation of apoptosis, migration and proliferation of pulmonary vascular cells. This leads to pulmonary vascular remodelling, resulting in PH, which is not spontaneously reversible. PH can ultimately lead to subsequent right heart failure. Pulmonary vascular alterations in hypoxia-induced PH are characterized by increased muscularization of small precapillary pulmonary arteries and stiffening of the large pulmonary arteries.[5] Mitochondria influence these processes by regulating intracellular calcium concentrations in PASMCs[7,8] and releasing mitochondrial reactive oxygen species (ROS)

that can activate ROS-sensitive ion channels,[9] as well as apoptosis[10,11] and transcription factors.[12]

Mitochondrial calcium and ROS release, as well as the induction of apoptosis, can be regulated by the mitochondrial proteins p66shc and CypD in response to strong stress stimuli. Phosphorylation of p66shc under conditions of cellular stress[13] induces its translocation into the mitochondria[14] where it is able to generate ROS.[15] The p66shc-induced ROS release increases the probability of mitochondrial permeability transition pore (mPTP) opening and regulates mitochondrial calcium release and apoptosis. The mPTP is located in the highly impermeable inner mitochondrial membrane and can operate in two different modes. Pulsatile low-conductance opening is thought to protect the mitochondria from hyperpolarisation and calcium overload, whereas high-conductance opening induces a ROS burst and the release of mitochondrial proteins into the cytosol, resulting in cell death.[16] The probability of mPTP opening can be enhanced by different signals, such as calcium and ROS, e.g., via activation of CypD. CypD is the mitochondrial isoform of cyclophilins[17] and covers an inhibitory binding site of the mPTP.[18] Although there is evidence that p66shc signalling may regulate proliferation,[19] the exact role of p66shc and CypD in the regulation of pulmonary vascular tone and remodelling is currently unknown. The role of p66shc-mediated ROS release in different systemic cardiovascular diseases has been recently reviewed.[20] P66shc may regulate pro-proliferative signalling via growth factor receptor-coupled pathways (for review see reference 21) while CypD might contribute to anti-proliferative signalling by controlling signal transducer and activator of transcription (STAT) 3-mediated inflammatory gene expression patterns.[22] We reasoned that p66shc and CypD might also play a role in cellular responses to physiologic stimuli, such as mild hypoxia, which might be different from their effects on cellular stress stimuli, such as ischaemia.

Against this background, we hypothesized that the regulation of calcium handling via p66shc and CypD can regulate pulmonary vascular function under physiological and pathophysiological conditions and that both proteins may act through common pathways.

2. Materials and methods

2.1 Animals

All animal experiments were approved by local governmental authorities (Regierungspräsidium Giessen) and were performed in accordance with the guidelines from Directive 2010/63/EU of the European Parliament on the protection of animals used for scientific purposes. The generation of mice deficient in p66shc,[14] CypD (lacking the *Ppif*-gene)[23] or both proteins[24] and their backcrossing on the C57BL/6J background were described previously. The mice were bred in the central animal facility of our university. C57BL/6J mice served as WT controls and were purchased from Charles River WIGA GmbH (Sulzfeld, Germany). Mice of both sexes were studied at 2–4 months of age.

2.2 Isolated, perfused, and ventilated mouse lungs

The lungs of WT, p66shc$^{-/-}$, CypD$^{-/-}$ and p66shc/CypD$^{-/-}$ mice were prepared and basal pulmonary arterial pressure (PAP) and HPV were determined as described previously.[25,26] Briefly, after anaesthetization by a single intraperitoneal injection of 2% xylazine hydrochloride (20 mg/kg body weight, Bela-pharm GmbH & Co. KG, Vechta, Germany) and 10% ketamine hydrochloride (100 mg/kg body weight, CEVA Tiergesundheit GmbH, Düsseldorf, Germany) and anticoagulation with heparin (50 000 I.U./kg bodyweight; Ratiopharm, Ulm, Germany), the animals were intubated and artificial ventilation started. After thoracotomy, catheters were placed and artificial perfusion with Krebs–Henseleit buffer was started. While isolating the heart–lung-convolute from the body, the perfusion rate and temperature were increased to 37°C and 2 mL/min, rinsing the lung of blood. Subsequently, the circuit was closed and the pressure was monitored. After 15 min of stable pressure, three repetitive hypoxic manoeuvres (1% O_2, 5.3% CO_2, balanced with N_2) and three bolus applications of 150 mM KCl (Merck KGaA, Darmstadt, Germany) to test vasoconstrictive ability were performed. For additional information and experiments, please refer to the Supplementary material online.

2.3 Quantification of hypoxia-induced PH

Mice were exposed to normobaric hypoxia (HOX; 10% O_2) or normoxia (NOX; 21% O_2) for four weeks in ventilated chambers (Biospherix, Ltd., Parish, USA). Transthoracic echocardiography was performed under anaesthesia, induced with 3% isoflurane and maintained via a nose cone with 1.5% isoflurane (balanced with O_2). Echocardiography was performed on Day 0 and Day 27 using a high-resolution imaging system, as described previously.[27–29]

The haemodynamic analysis was performed using a microtip catheter (SPR-671NR; ADInstruments, Dunedin, New Zealand), as described previously.[27] Briefly, the mice were anaesthetized with xylazine 2% hydrochloride and 10% ketamine hydrochloride by a single intraperitoneal injection, followed by intubation and ventilation with O_2. While maintaining the body temperature at 37°C, the pressure of the right ventricle (RV) and the aorta were recorded. The mice were subsequently sacrificed by exsanguination.

Changes in heart morphology were determined by dissecting the free wall of the RV from the left ventricle and septum (LV+S). The heart ratio (Fulton's index) was calculated by dividing the RV by (LV+S) mass; changes in the left heart morphology were assessed by dividing the LV mass by the bodyweight in g.

2.4 Vascular remodelling, passive vessel function, and density of the pulmonary vasculature

Blinded analysis of muscularization was performed as described previously.[27,30] Briefly, for histological examination, directly after exsanguination the lungs were flushed and fixed with formalin. The pulmonary vessels were double-stained with anti-α-smooth muscle actin antibody (1:900 dilution, clone 1A4, Sigma-Aldrich, Saint Louis, USA) and human anti-von Willebrand factor antibody (1:900 dilution, Dako, Hamburg, Germany), followed by counterstaining with methyl green. The degree of muscularization of the small peripheral pulmonary vessels was determined by using a computerized morphometric system (Qwin, Leica, Wetzlar, Germany). The percentages of non-, partially, and fully muscularized vessels were calculated by dividing the number of vessels in the category by the total number counted. All vessels were analysed. For representative images, please refer to the Supplementary material online, *Figure S5A–C.*

To determine alterations of the passive vessel function (stiffness), left and right pulmonary artery rings were isolated directly after exsanguination and analysed by a wire myograph (Multimyograph 620 M; Danish MyoTechnology A/S, Arhus, Denmark). The experiments were performed according to a previously described protocol.[31,32] Briefly, the samples were mounted and equilibrated in a physiological salt solution (PSS), a wake-up protocol was applied, and finally, the buffer was changed to calcium-free PSS. The distance between the wires was enlarged stepwise, and the force was recorded in LabChart (ADInstruments, Dunedin, New Zealand). Using regression analysis, the stress–strain curve displaying the relationship between the logarithmically transformed resting wall tension and the corresponding internal diameter was determined.[33] The density of the pulmonary vasculature was determined by lung vessel casting with Microfil® (Flow Tech, Inc., Carver, Massachusetts) and subsequent *ex vivo* µCT imaging. Please refer to the Supplementary material online for details.

2.5 PASMC isolation

Mouse precapillary PASMCs were isolated and cultured as described previously.[26,34] Briefly, the mice were deeply anaesthetized by intraperitoneal injection of 2% xylazine hydrochloride (20 mg/kg body weight) and 10% ketamine hydrochloride (100 mg/kg body weight) and anticoagulated with heparin (50 000 I.U. heparin/kg body weight). The mice were subsequently sacrificed by exsanguination according to the approved animal care and use protocols. The lungs were rinsed, and a mixture containing 0.5% low-melting point agarose (type VII, Sigma-Aldrich, Munich, Germany) and 0.5% Fe_3O_4 particles (Sigma-Aldrich, Munich, Germany) was delivered via the RV. After chopping and shearing, tissue particles containing iron were separated using a magnet. The particles were then resuspended and transferred to cell culture dishes for culturing PASMCs.

2.6 Calcium imaging

PASMCs were cultured on coverslips loaded with 5 µm Fura-2-AM (Sigma-Aldrich, Steinheim, Germany) and were analysed as described

previously.[26] Fura-2 is excited at 340 nm (Ca^{2+} bound) and 380 nm (Ca^{2+} free). In both states, the emission is 510 nm. The 340/380 nm ratio is related to the concentration of intracellular calcium ($[Ca^{2+}]_i$). The basal $[Ca^{2+}]_i$ and the increase after stimulation with 0.4 M KCl were investigated.

2.7 Calcium-induced mPTP opening in isolated lung mitochondria and mitochondrial calcium imaging

Please refer to Supplementary material online.

2.8 Western blot analysis

Proteins were isolated from lung homogenates of C57BL/6J mice after normoxic and chronic hypoxic (10% O_2 for 4 weeks) exposure. Rabbit anti-shc (1:1000 dilution, BD-Transduction, Heidelberg, Germany), mouse anti-cyclophilin F (1:1000 dilution, Abcam, Cambridge, Great Britain), and anti-β-actin (1:50 000 dilution, Sigma-Aldrich, Munich, Germany) were used as primary antibodies for protein detection.

2.9 Real-time quantitative polymerase chain reaction analysis

PCR analysis was performed as previously described.[35] RNA was extracted from lung homogenates by using an RNeasy Mini Kit (Qiagen N.V., Hilden, Germany) and reverse-transcribed using an iScript cDNA Synthesis Kit (Bio-Rad, Berkeley, California). Total cDNA was used to perform quantitative real-time PCR using an RT-PCR master mix (iTaq SYBR Green Supermix with ROX, Bio-Rad, Berkeley, CA, USA). Real-time quantitative polymerase chain reaction (RT-PCR) was performed in a CFX Connect™ Real-Time PCR Detection System (Bio-Rad Laboratories, Inc.). β2-microglobulin was used as a reference gene. Primers are listed in the Supplementary material online.

2.10 Statistics

The statistical analysis of linear models was performed using 'R' ('R' Foundation for Statistical Computing, Vienna, Austria). For isolated lung experiments, statistical significance for multiple-to-one comparisons was calculated using Dunnett's multiple comparison procedure. Tukey's honestly significant difference test was used for all pairwise comparisons in the hypoxia-induced PH experiments. Student's *t*-test was used for simple comparisons of two groups. For outlier analysis, ROUT method was used. The figures were created using GraphPad Prism 6.0 (GraphPad Software, Inc.; La Jolla, USA) or 'R'.

3. Results

3.1 Pulmonary p66shc protein expression was significantly upregulated after chronic exposure to hypoxia

Protein expression was determined in the lung homogenates of WT mice after exposure to chronic hypoxia (4 weeks, 10% O_2). The p66shc protein content was elevated in hypoxic samples, but the CypD content was unaltered (*Figure 1A,B*). Interestingly, both CypD and p66shc mRNA expression was unchanged in the hypoxic lung homogenates (*Figure 1C,D*). At the cellular level, the content of p66shc protein in PASMCs was unaltered by exposure to hypoxia, while the content in endothelial cells (ECs) was upregulated. CypD protein expression was downregulated in PASMCs but upregulated in ECs (*Figure 1E,F*). As the

main site of action of p66shc is at the inner mitochondrial membrane, subcellular fractionation was performed to verify that p66shc was translocated to the mitochondria (Supplementary material online, *Figure S1*).

3.2 Mice deficient in p66shc and/or CypD had a lower right ventricular systolic pressure (RVSP) than WT mice but a similar response to chronic hypoxia

RVSP was decreased to a similar extent in mice deficient in p66shc, CypD or both proteins after normoxic or hypoxic (4 weeks, 10% O_2) exposure compared to WT mice. All mouse strains showed an increase in RVSP after chronic hypoxic exposure to a similar extend (*Figure 2A*). The systemic arterial pressure (SAP) was unaltered by hypoxic exposure but was significantly reduced in mice deficient in CypD under basal conditions (*Figure 2B*). Original tracings are shown in *Figure 2G*.

3.3 Cardiac remodelling and function was not altered by p66shc and/or CypD genetic deficiency

To decipher whether the differences in RVSP were related to differences in heart function or structure, we next performed cardiac morphometry and echocardiography. The ratio of the right ventricular (RV) mass to left ventricular (LV) mass plus septum (heart ratio) was not influenced by the genotype and increased after exposure to chronic hypoxia in all mouse strains to a similar degree (*Figure 2C*). Although CypD$^{-/-}$ mice showed a lower SAP, there were no differences in the weight of the left ventricle plus septum corrected for the bodyweight (LV + septum/BW in mg/g) (*Figure 2D*).

The echocardiographic analysis showed a decreased cardiac index (CI) after exposure to hypoxia, but there were no differences between the mouse strains (*Figure 2E*). Tricuspid annular plain systolic excursion (TAPSE), a parameter for the systolic function of the RV, showed the expected decrease in hypoxic animals, but again there were no differences between the mouse strains (*Figure 2F*).

3.4 Pulmonary vascular remodelling and the proliferation of PASMCs were not affected by the different genotypes

Morphometric analysis of the small pulmonary arteries was performed to determine the degree of vascular muscularization. A higher portion of fully muscularized vessels, and a lower portion of partially and non-muscularized vessels, were detected after chronic hypoxic exposure, indicating significant vascular remodelling in hypoxic lungs. However, for vessels with a diameter of 20–70 µm, there were no significant differences in the extent of remodelling when comparing non-, partially, and fully muscularized vessels between different genotypes (*Figure 3A*). A more detailed visualization of the results showing the degree of muscularization in % is displayed in Supplementary material online, *Figure S5D*. Accordingly, the proliferation of PASMCs was unchanged when comparing the different genotypes (Supplementary material online, *Figure S4A*). The stiffness of the left and right pulmonary arteries was significantly increased by exposure to chronic hypoxia. The left pulmonary artery showed a higher stiffness compared to the right pulmonary artery. However, no significant differences between the genotypes were detected (*Figure 3B*). Furthermore, we detected no difference in vascular density in the different genotypes measured by µCT (*Figure 3C,D*). To quantify fibrosis, we measured the amount of collagen deposition in lung
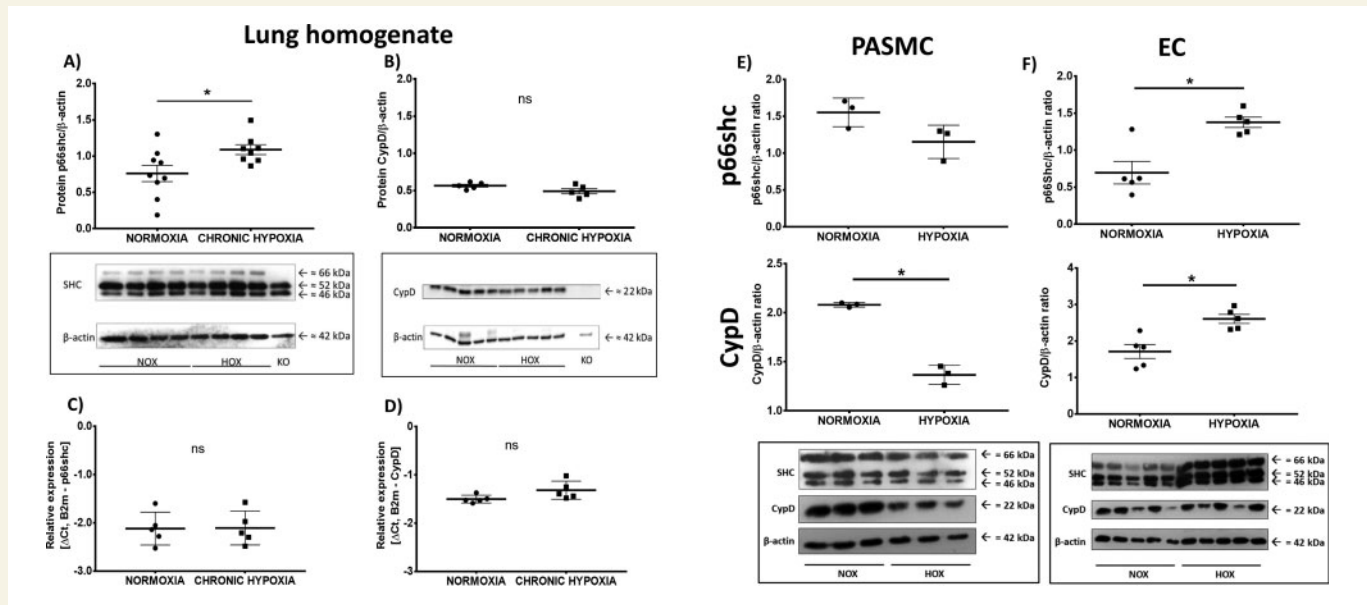
Figure 1. Expression of p66shc and cyclophilin D (CypD) in lung tissue (*A–D*) after exposure to chronic hypoxia (10% O_2; 4 weeks), and pulmonary arterial smooth muscle cells (PASMCs; *E*) or endothelial cells (ECs; *F*) of wild-type (WT) mice after a 5-day exposure to hypoxia. (*A*) Protein expression was determined with an antibody against SH2 containing proto-oncogene (shc) proteins p66shc, p52shc, and p46shc. P66shc expression was compared to β-actin expression. Lung homogenate from p66shc$^{-/-}$ mice (KO) was used as negative control (*n* = 9, from two western blots, one *n* excluded after outlier analysis). A representative western blot is shown. (*B*) Protein expression of CypD compared to β-actin expression. Lung homogenate from CypD$^{-/-}$ mice was used as negative control (*n* = 5). A representative western blot is shown. (*C*) Expression of p66shc mRNA compared to the expression of the reference gene (β2-microglobulin) in lung homogenate of WT mice (*n* = 5). (*D*) Expression of CypD mRNA compared to the expression of the reference gene (β2-microglobulin) in lung homogenate of WT mice (*n* = 5). (*E*) Protein expression in PASMCs determined with an antibody against cyclophilin D or SH2 containing proto-oncogene (shc) proteins p66shc, p52shc, and p46shc. Expression was compared to β-actin expression. *n* = 3 individual cell isolations. A representative western blot is shown. (*F*) Protein expression in ECs determined with an antibody against cyclophilin D or SH2 containing proto-oncogene (shc) proteins p66shc, p52shc, and p46shc. Expression was compared to β-actin expression. *n* = 5 individual cell isolations, one *n* excluded for quantitative analysis according to outlier analysis. A representative western blot is shown. * $P < 0.05$, determined by *t*-test. Data are shown as the mean ± SEM after outlier analysis.

slices and did not detect any significant differences between the genotypes (Supplementary material online, *Figure 5E*).

3.5 Normoxic PAP and vasoreactivity was decreased in isolated lungs of gene-deficient mice

Normoxic PAP was lower in mice lacking p66shc, CypD or both proteins when compared to WT controls but did not differ between the respective knockout mice (*Figure 4A*).

The KCl- and phenylephrine (PE)-induced vasoconstriction were also lower in lungs from knockout mice compared to WT, but again they did not differ between the different knockout mice (*Figure 4B,C*). Representative tracings of PAP measurements are displayed in *Figure 4D*.

While acute HPV was decreased in lungs from p66shc$^{-/-}$, CypD$^{-/-}$, and p66shc/CypD$^{-/-}$ mice compared to WT lungs (*Figure 4E,F*), sustained HPV was not affected by the genotype (*Figure 4F*). When comparing the relative intracellular calcium contents of PASMCs (*Figure 5A*), no differences were found between the different knockout and WT cells at the basal level. The absolute calcium concentrations in WT PASMCs are provided in Supplementary material online, *Figure 3B*. However, the increase of [Ca^{2+}]$_i$ in response to KCl application was decreased in PASMCs from gene-deficient lungs (*Figure 5B*). Given that H_2O_2 (amongst other ROS) has been suggested as a downstream messenger

in HPV,[3] we quantified the basal and cytosolic H_2O_2 concentration by HyPer$_{cyto}$ in PASMCs. We found no significant differences between the genotypes in baseline fluorescence. After stimulation with 0.4 M KCl, the H_2O_2 concentration was unchanged in WT PASMCs compared to knockout PASMCs (Supplementary material online, *Figure S2*). As the content and activity of various ion channels are crucial for vasoconstriction, the mRNA expression of various ion channels contributing to calcium homeostasis was analysed; however, no significant differences were detected (Supplementary material online, *Figure S4B*).

3.6 Mitochondrial calcium retention capacity and potassium chloride-induced calcium increase was enhanced in CypD$^{-/-}$ and CypD/p66shc$^{-/-}$ but not in p66shc$^{-/-}$ mitochondria

Mitochondrial calcium retention capacity (CRC) determined by measurement of mitochondrial calcium uptake during stepwise increase of extramitochondrial calcium concentration was augmented in isolated mitochondria of CypD$^{-/-}$ and CypD/p66shc$^{-/-}$ compared to WT and

p66shc$^{-/-}$ mice (*Figure 5C*), indicating that mPTP opening is delayed by CypD knockout. Accordingly, inhibition of mPTP opening by cyclosporine A (CsA) increased CRC to similar levels in all genotypes (*Figure 5D*).
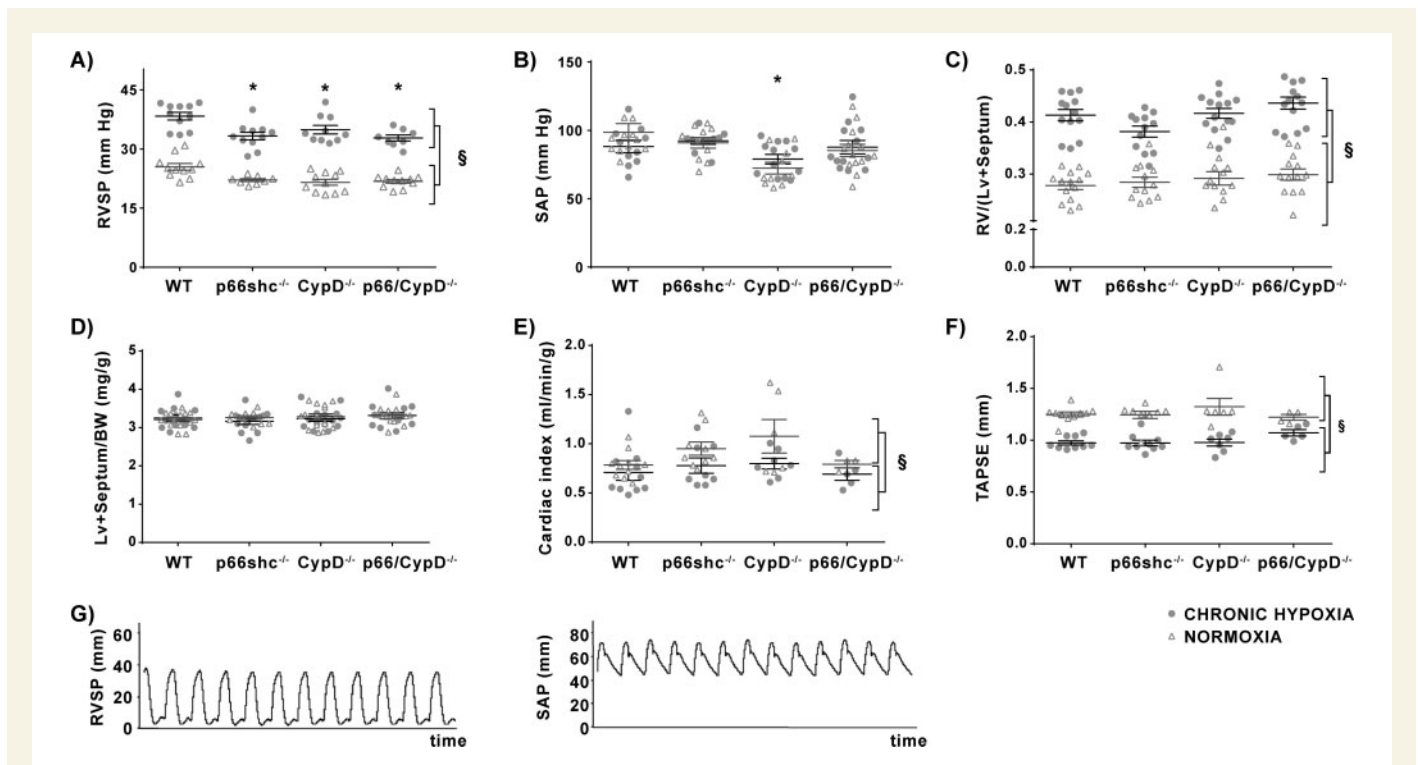
Figure 2. Haemodynamic and cardiac parameters in p66shc$^{-/-}$, CypD$^{-/-}$, p66shc/CypD$^{-/-}$, and WT mice after 4 weeks of exposure to hypoxia or normoxia. (A) Right ventricular systolic pressure (RVSP) in mmHg (n = 8–11 mice per group). (B) Systemic arterial pressure (SAP) in mmHg (n = 10–13 mice per group). (C) Right heart hypertrophy given as the ratio of the right ventricular mass (RV) to left ventricular plus septal mass (LV+septum) (n = 12–14 mice per group). (D) Mass of LV+septum compared to body weight (n = 17–20 mice per group). (E) Heart function given as cardiac index (CI = cardiac output/body weight) measured by echocardiography (n = 3–10 mice per group). (F) Systolic function of the RV given as tricuspid annular plane systolic excursion (TAPSE) in mm (n = 4–10 mice per group). (G) Original tracings of right ventricular systolic pressure (RVSP) in mmHg (left) and systolic arterial pressure (SAP) in mmHg (right) from a wild-type animal after exposure to chronic hypoxia (10%, 4 weeks). § $P < 0.01$, main effect of exposure and genotype in a two-factorial model; * $P < 0.05$ Tukey's honestly significant difference test compared to wild-type mice. Data are shown as the mean ± SEM.

4. Discussion

In line with these results, the KCl-induced mitochondrial calcium increase was enhanced in isolated PASMCs from CypD$^{-/-}$ and CypD/p66shc$^{-/-}$ compared to WT and p66shc$^{-/-}$ mice (*Figure 5E,F*).

Our study shows that the mitochondrial proteins p66shc and CypD affect pulmonary vascular contractility, but we did not detect differences in pulmonary vascular remodelling or a specific contribution to hypoxia-induced responses of the pulmonary vasculature. These conclusions are based on the findings that (i) the pulmonary vascular pressure was decreased in gene-deficient mice compared to WT mice *in vivo* and in isolated lungs, (ii) the chronic hypoxia-induced alterations were similar among the different genotypes, and (iii) acute HPV and the PE- and KCl-induced pulmonary vasoconstriction were decreased in gene-deficient mice. The decreased basal pulmonary vascular tone was most likely caused by a change in calcium-dependent vasoconstriction rather than by morphological differences in the pulmonary vascular bed or alterations in heart function. This conclusion is based on the fact that neither pulmonary vascular remodelling, pulmonary arterial stiffness, or vascular density, nor cardiac function was changed in the knockout mice, but KCl-stimulated intracellular calcium levels were significantly reduced in

PASMC of gene-deficient mice. Moreover, KCl-induced mitochondrial calcium uptake was attenuated in mice lacking CypD indicating that only CypD regulates intracellular calcium levels and vascular contractility via interference with mitochondrial calcium homeostasis. While the effect of p66shc$^{-/-}$ was specific for the pulmonary vasculature, CypD$^{-/-}$ also decreased systemic pressure. Thus, p66shc and CypD regulate the physiological tone of pulmonary vessels, but not their specific response to mild hypoxia.

Our findings are in line with previous studies showing that p66shc and CypD proteins can affect cellular calcium homeostasis in non-pulmonary cells. While the high concentrations of ROS released by p66shc may activate the mPTP to induce apoptosis,[15] small amounts of ROS can induce low-conductance opening of the mPTP[16] to release mitochondrial calcium from the matrix. mPTP activation can occur due to strong stress stimuli, e.g., through the interaction of ROS and CypD, which leads to the blockage of an mPTP inhibitory site.[23] Thus, gene deficiency of p66shc and CypD can be expected to result in decreased mitochondrial calcium release and decreased cytosolic calcium concentration. Previous studies have shown that the ablation of CypD results in calcium sequestration in non-pulmonary mitochondria in adult rat and mouse ventricular cardiomyocytes, which probably leads to reduced cytosolic calcium levels.[36–38] We were able to show for the first time in lung mitochondria and isolated PASMCs that increased mitochondrial calcium sequestering
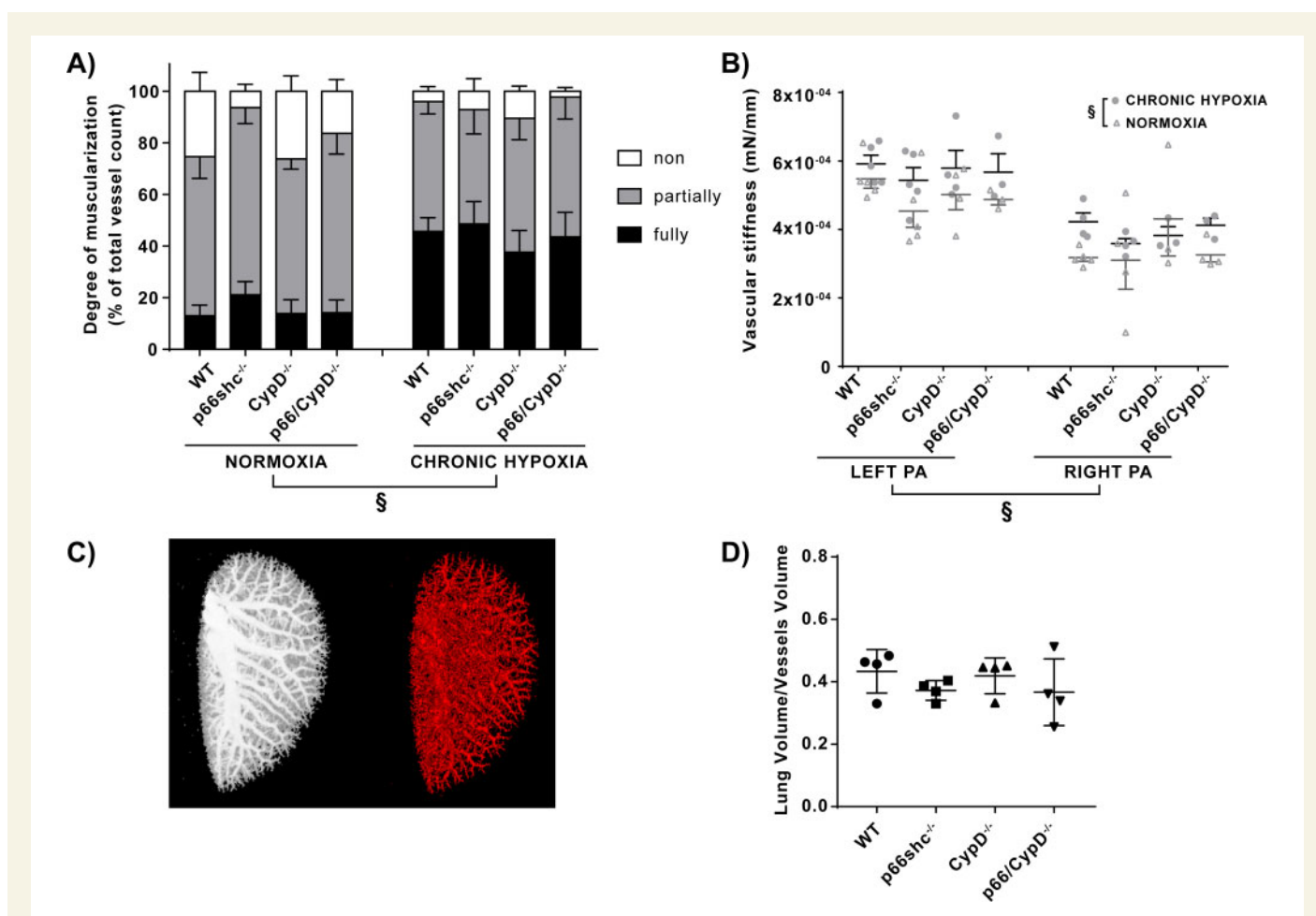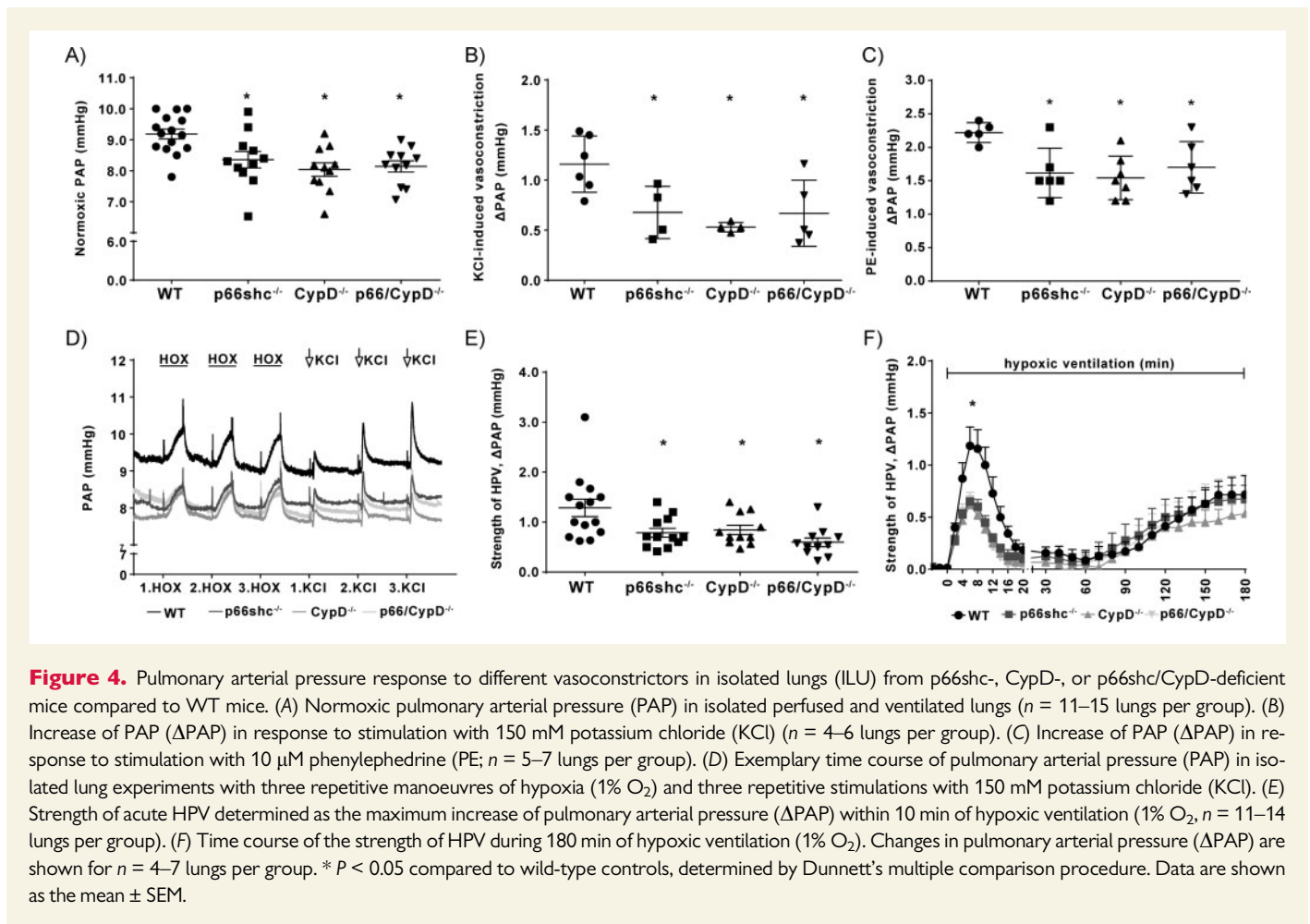
Figure 3. Remodelling of small and large pulmonary arteries and density of the pulmonary vasculature in p66shc^{-/-}, CypD^{-/-}, p66shc/CypD^{-/-}, and WT mice after 4 weeks of exposure to hypoxia or normoxia. (*A*) Degree of muscularisation of small pulmonary arteries. Shown is the fraction of fully, partially, and non-muscularized vessels in % of all analysed vessels (*n* = 4–6 mice per group). § *P* < 0.01, difference in the proportion of fully, partially and non-muscularised vessels, analysed by a two-factorial model of exposure and genotype. (*B*) Stiffness of the large extrapulmonary arteries analysed for the left and right pulmonary artery (PA) of the respective groups. The stiffness is displayed as the tangential slope of the determined stress–strain curve in mN/mm (*n* = 3–6 arteries per group). § *P* < 0.01, determined by a two-factorial model of exposure and genotype, adjusted for the site of collection (left/right PA). (*C*) Representative μCT images of the vascular tree of the left lungs after *ex vivo* Microfil® application. Left: Maximum intensity projection. Right: Reconstructed segmented pulmonary vasculature. (*D*) Data from (*C*), presented as ratio of total lung volume to volume of lung vasculature (*n* = 4 mice per group). No significant difference compared to WT mice was detected with Dunnett's multiple comparison procedure. Data are shown as the mean ± SEM.

in CypD^{-/-} cells does not only occur under strong stress stimuli, such as mitochondrial calcium overload, leading to mPTP opening, but also under more physiologic conditions like stimulation with KCl and thus can regulate physiologic cytosolic calcium levels. In contrast, we did not detect alterations of mitochondrial calcium handling in p66shc^{-/-} mice as an underlying reason for changes in intracellular calcium concentrations. These findings suggest that besides exerting mitochondrial effects, cytosolic p66shc can possibly regulate cellular calcium handling by affecting cytosolic kinases or the cytosolic ROS production e.g. via cytosolic NADPH-oxidases,[39] although we did not detect significant differences in intracellular hydrogen peroxide levels in PASMCs of the different genotypes. The modulation of KCl-induced intracellular calcium peaks in PASMCs by CypD and p66shc are sufficient to explain the altered contractility in isolated lungs, as KCl and also acute hypoxia are known to exert their contractile effects in PASMCs by increasing the intracellular calcium concentration[40,41] and at least KCl-induced vasoconstriction is not affected by pulmonary endothelium-related regulation of vasoconstriction. As the basal intracellular calcium concentration was not altered in gene-deficient PASMCs, it seems unlikely that the knockout of CypD or p66shc interferes with calcium clearance mechanisms, such as sarcoplasmic/endoplasmic reticulum calcium ATPase. Thus, in the presence of local vasoconstrictive stimulators, which continuously balance basal pulmonary vascular pressure, also basal vascular tone *in vivo* and in the isolated organ may be affected by differential calcium handling processes in knockout vs. WT PASMCs.[42] In contrast to acute HPV, sustained HPV may be predominantly executed through sensitizing effects of the contractile apparatus,[43] which would explain why we did not detect differences in the strength of HPV during sustained hypoxia in the different genotypes. This finding thus supports previous studies that have reported the differential regulation of acute and sustained HPV and chronic hypoxia.[5,6]

We did not find any evidence for additional morphologic mechanisms underlying the decreased vascular tone, as the degree of muscularization, vessel stiffness and vascular density was not influenced by the genotype.

Figure 4. Pulmonary arterial pressure response to different vasoconstrictors in isolated lungs (ILU) from p66shc-, CypD-, or p66shc/CypD-deficient mice compared to WT mice. (*A*) Normoxic pulmonary arterial pressure (PAP) in isolated perfused and ventilated lungs (*n* = 11–15 lungs per group). (*B*) Increase of PAP (ΔPAP) in response to stimulation with 150 mM potassium chloride (KCl) (*n* = 4–6 lungs per group). (*C*) Increase of PAP (ΔPAP) in response to stimulation with 10 μM phenylephredine (PE; *n* = 5–7 lungs per group). (*D*) Exemplary time course of pulmonary arterial pressure (PAP) in isolated lung experiments with three repetitive manoeuvres of hypoxia (1% O$_2$) and three repetitive stimulations with 150 mM potassium chloride (KCl). (*E*) Strength of acute HPV determined as the maximum increase of pulmonary arterial pressure (ΔPAP) within 10 min of hypoxic ventilation (1% O$_2$, *n* = 11–14 lungs per group). (*F*) Time course of the strength of HPV during 180 min of hypoxic ventilation (1% O$_2$). Changes in pulmonary arterial pressure (ΔPAP) are shown for *n* = 4–7 lungs per group. * *P* < 0.05 compared to wild-type controls, determined by Dunnett's multiple comparison procedure. Data are shown as the mean ± SEM.

The finding that the right and left PA showed differing stiffness might be related to their different morphology and was described previously.[44]

The p66shc and CypD proteins are expressed in heart and lung tissue.[45,46] However, as cardiac function was not affected by the genotype, and heart function does not influence haemodynamics in isolated lung experiments, we can exclude the possibility that cardiac effects contributed to the observed differences. Thus, our results suggest that acute vasoreactivity and the basal vascular tone are decreased in p66shc- and CypD-deficient lungs due to the regulation of intracellular PASMC calcium homeostasis; in the case of CypD$^{-/-}$ probably via mitochondrial calcium sequestration.

Interestingly, we did not detect any differences in the hypoxic responses between the genotypes. Although isolated lungs of the gene-deficient mice had a lower response to acute hypoxia compared to WT lungs, this effect was not specific for hypoxia, as non-hypoxic vasoconstriction induced by KCl was also decreased. Moreover, we did not detect differences between the mouse lines with regard to the chronic hypoxia-induced increase of pulmonary vascular pressure, right heart hypertrophy or vascular remodelling. Such differences were however, expected, as p66shc and CypD are involved in the regulation of cellular calcium concentrations, ROS, proliferation, and the induction of apoptosis,[14,47] factors contributing to the development of pulmonary vascular remodelling in hypoxia.[5] Interestingly, we found a cell-type-specific regulation of p66shc and CypD in chronic hypoxic pulmonary cells; however, the physiological relevance of increased hypoxia-induced expression in

endothelial cells still needs to be determined. The hypoxia-dependent regulation of p66shc obviously occurs at the protein level because its mRNA expression was not significantly altered by hypoxia. These alterations should be investigated in future studies.

With regard to the effect of CypD and p66shc deficiency on cardiac function, our findings are in line with previous studies that also did not detect differences of cardiac function in the knockout compared to WT mice under baseline conditions.[38,48] However, p66shc or CypD gene deficiency also did not affect right ventricular cardiac remodelling or function after exposure to chronic hypoxia, although an effect of p66shc or CypD gene deletion in left heart hypertrophy models has been reported. While p66shc-deficient mice were partially protected from left heart hypertrophy and apoptosis of myocytes,[48] CypD$^{-/-}$ mice showed more severe heart hypertrophy and a lower functional cardiac reserve during increased left heart afterload.[38] This finding could be explained by the altered function of the right heart in a low-pressure system and its different ontogenetic origin.[49,50] p66shc and CypD obviously exerted different functions in right and left heart hypertrophy; however, the effects might be related to the differences between hypoxia-induced and afterload-induced models.

Interestingly, the mice deficient for both proteins did not differ in their pulmonary vascular tone from the mice lacking only one protein. This suggests that both proteins regulate pulmonary vascular tone through similar signalling pathways. This suggestion is in line with a previous study in which double-knockout mice also did not show additive effects in a
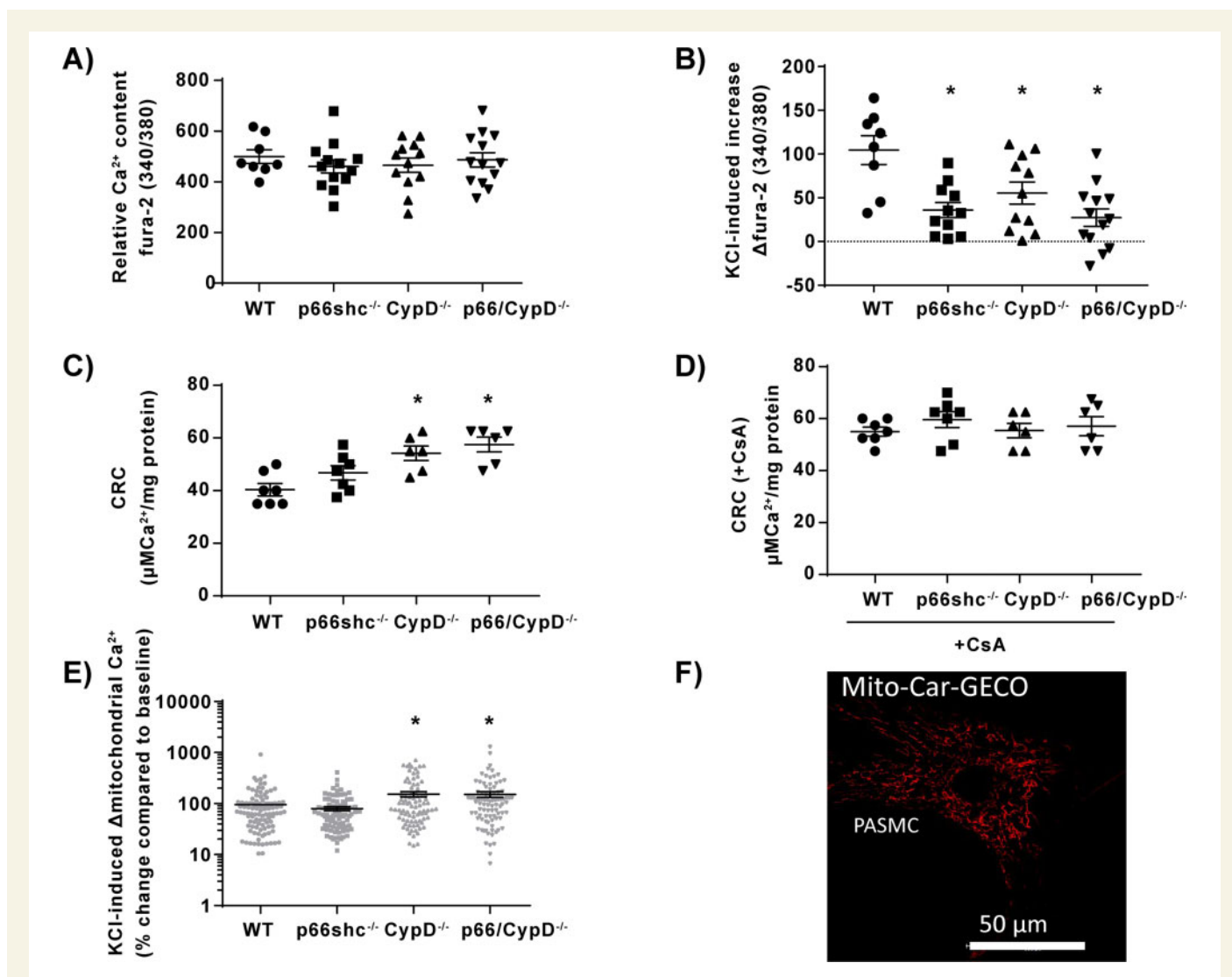
Figure 5. Calcium handling in isolated pulmonary mitochondria and pulmonary arterial smooth muscle cells (PASMCs) from p66shc-, CypD-, and p66shc/CypD-deficient mice compared to WT mice. (A) Relative basal intracellular calcium content (Ca^{2+}) of PASMCs quantified as the fura-2-fluorescence ratio of 340–380 nm during normoxia ($n = 8$–13 experiments from four cell isolations). (B) Increase of relative intracellular calcium content of PASMCs quantified as the fura-2-fluorescence ratio of 340–380 nm in response to KCl stimulation in PASMCs ($n = 8$–13 experiments from four cell isolations). (C) Calcium retention capacity (CRC) given as amount of calcium (Ca^{2+}) per mg mitochondrial protein required to induce mPTP opening, detected as sudden increase in extramitochondrial calcium with calcium green 5 N fluorescence ($n = 6$–7 experiments, each from an individual cell isolation). (D) Calcium retention capacity (CRC) given as amount of calcium (Ca^{2+}) per mg mitochondrial protein required to induce mPTP opening, detected as sudden increase in extramitochondrial calcium with calcium green 5 N fluorescence in presence of 1 μM of the mPTP inhibitor cyclosporin A (CsA) ($n = 6$–7 experiments, each from an individual cell isolation) (E) Mitochondrial calcium increase determined with Mito-Car-GECO in intact PASMCs after stimulation with 50 mM KCl detected as % change compared to baseline fluorescence ($n = 10$ experiments from three individual cell isolations). (F) Representative picture of PASMCs transfected with the genetically encoded dye Mito-Car-GECO; 590 nm and 620–640 nm were used for excitation and emission. *$P < 0.05$ compared to wild-type controls determined by Dunnett's multiple comparison procedure. Data are shown as the mean ± SEM.

model of experimental autoimmune encephalitis. The authors concluded that the proteins are epistatic and that, in contrast to our findings, p66shc and CypD exerted their effects by activating mPTP opening.[24]

Importantly, the systemic pressure was also decreased in CypD^{-/-} mice but not in p66shc^{-/-} mice, which might qualify p66shc as a therapeutic target for pulmonary vascular diseases. This specific effect on the pulmonary vasculature may be a result of the different expression levels of p66shc in the pulmonary vs. the systemic circulation; it has been shown

that the protein levels of p66shc in the lungs of adult mice are higher than those in the heart, kidney, and liver.[45]

In conclusion, our study is the first to describe the role of p66shc and CypD in the regulation of pulmonary vascular tone. Furthermore, we show for the first time that CypD can regulate mitochondrial and cytosolic calcium levels in PASMCs in response to a physiologic vasoconstrictive stimulus. Interestingly, neither p66shc nor CypD was specifically involved in the hypoxic responses of the pulmonary vasculature.

Supplementary material

Supplementary material is available at *Cardiovascular Research* online.

Data availability statement

All data are incorporated into the article and its online supplementary material.

References

1. Rizzuto R, De Stefani D, Raffaello A, Mammucari C. Mitochondria as sensors and regulators of calcium signalling. *Nat Rev Mol Cell Biol* 2012;**13**:566–578.
2. Salvaterra CG, Goldman WF. Acute hypoxia increases cytosolic calcium in cultured pulmonary arterial myocytes. *Am J Physiol* 1993;**264**:L323–328.
3. Sommer N, Strielkov I, Pak O, Weissmann N. Oxygen sensing and signal transduction in hypoxic pulmonary vasoconstriction. *Eur Respir J* 2016;**47**:288–303.
4. Euler USv, Liljestrand G. Observations on the pulmonary arterial blood pressure in the cat. *Acta Physiol* 1946;**12**:301–320.
5. Wilkins MR, Ghofrani HA, Weissmann N, Aldashev A, Zhao L. Pathophysiology and treatment of high-altitude pulmonary vascular disease. *Circulation* 2015;**131**:582–590.
6. Robertson TP, Ward JP, Aaronson PI. Hypoxia induces the release of a pulmonary-selective, Ca(2+)-sensitising, vasoconstrictor from the perfused rat lung. *Cardiovasc Res* 2001;**50**:145–150.
7. Undem C, Luke T, Shimoda LA. Contribution of elevated intracellular calcium to pulmonary arterial myocyte alkalinization during chronic hypoxia. *Pulm Circ* 2016;**6**:93–102.
8. Lai N, Lu W, Wang J. Ca(2+) and ion channels in hypoxia-mediated pulmonary hypertension. *Int J Clin Exp Pathol* 2015;**8**:1081–1092.
9. Veit F, Pak O, Brandes RP, Weissmann N. Hypoxia-dependent reactive oxygen species signaling in the pulmonary circulation: focus on ion channels. *Antioxid Redox Signal* 2015;**22**:537–552.
10. Kuo CY, Chiu YC, Lee AY, Hwang TL. Mitochondrial Lon protease controls ROS-dependent apoptosis in cardiomyocyte under hypoxia. *Mitochondrion* 2015;**23**:7–16.
11. Zhang L, Ma C, Zhang C, Ma M, Zhang F, Zhang L, Chen Y, Cao F, Li S, Zhu D. Reactive oxygen species effect PASMCs apoptosis via regulation of dynamin-related protein 1 in hypoxic pulmonary hypertension. *Histochem Cell Biol* 2016;**146**:71–84.
12. Chandel NS, Maltepe E, Goldwasser E, Mathieu CE, Simon MC, Schumacker PT. Mitochondrial reactive oxygen species trigger hypoxia-induced transcription. *Proc Natl Acad Sci USA* 1998;**95**:11715–11720.
13. Pinton P, Rimessi A, Marchi S, Orsini F, Migliaccio E, Giorgio M, Contursi C, Minucci S, Mantovani F, Wieckowski MR, Del Sal G, Pelicci PG, Rizzuto R. Protein kinase C beta and prolyl isomerase 1 regulate mitochondrial effects of the life-span determinant p66Shc. *Science* 2007;**315**:659–663.
14. Migliaccio E, Giorgio M, Mele S, Pelicci G, Reboldi P, Pandolfi PP, Lanfrancone L, Pelicci PG. The p66shc adaptor protein controls oxidative stress response and life span in mammals. *Nature* 1999;**402**:309–313.
15. Giorgio M, Migliaccio E, Orsini F, Paolucci D, Moroni M, Contursi C, Pelliccia G, Luzi L, Minucci S, Marcaccio M, Pinton P, Rizzuto R, Bernardi P, Paolucci F, Pelicci PG. Electron transfer between cytochrome c and p66Shc generates reactive oxygen species that trigger mitochondrial apoptosis. *Cell* 2005;**122**:221–233.
16. Brenner C, Moulin M. Physiological roles of the permeability transition pore. *Circ Res* 2012;**111**:1237–1247.
17. Connern CP, Halestrap AP. Purification and N-terminal sequencing of peptidyl-prolyl cis-trans-isomerase from rat liver mitochondrial matrix reveals the existence of a distinct mitochondrial cyclophilin. *Biochem J* 1992;**284**: 381–385.
18. Di Lisa F, Carpi A, Giorgio V, Bernardi P. The mitochondrial permeability transition pore and cyclophilin D in cardioprotection. *Biochim Biophys Acta* 2011;**1813**:1316–1322.
19. Frijhoff J, Dagnell M, Augsten M, Beltrami E, Giorgio M, Ostman A. The mitochondrial reactive oxygen species regulator p66Shc controls PDGF-induced signaling and migration through protein tyrosine phosphatase oxidation. *Free Radic Biol Med* 2014;**68**:268–277.
20. Di Lisa F, Giorgio M, Ferdinandy P, Schulz R. New aspects of p66Shc in ischaemia reperfusion injury and other cardiovascular diseases. *Br J Pharmacol* 2017;**174**:1690–1703.
21. Bhat SS, Anand D, Khanday FA. p66Shc as a switch in bringing about contrasting responses in cell growth: implications on cell proliferation and apoptosis. *Mol Cancer* 2015;**14**:76.
22. Tavecchio M, Lisanti S, Lam A, Ghosh JC, Martin NM, O'Connell M, Weeraratna AT, Kossenkov AV, Showe LC, Altieri DC. Cyclophilin D extramitochondrial signaling controls cell cycle progression and chemokine-directed cell motility. *J Biol Chem* 2013;**288**:5553–5561.
23. Basso E, Fante L, Fowlkes J, Petronilli V, Forte MA, Bernardi P. Properties of the permeability transition pore in mitochondria devoid of Cyclophilin D. *J Biol Chem* 2005;**280**:18558–18561.
24. Savino C, Pelicci P, Giorgio M. The P66Shc/mitochondrial permeability transition pore pathway determines neurodegeneration. *Oxid Med Cell Longev* 2013;**2013**:1–7.
25. Weissmann N, Manz D, Buchspies D, Keller S, Mehling T, Voswinckel R, Quanz K, Ghofrani HA, Schermuly RT, Fink L, Seeger W, Gassmann M, Grimminger F. Congenital erythropoietin over-expression causes "anti-pulmonary hypertensive" structural and functional changes in mice, both in normoxia and hypoxia. *Thromb Haemost* 2005;**94**:630–638.
26. Weissmann N, Dietrich A, Fuchs B, Kalwa H, Ay M, Dumitrascu R, Olschewski A, Storch U, Mederos y Schnitzler M, Ghofrani HA, Schermuly RT, Pinkenburg O, Seeger W, Grimminger F, Gudermann T. Classical transient receptor potential channel 6 (TRPC6) is essential for hypoxic pulmonary vasoconstriction and alveolar gas exchange. *Proc Natl Acad Sci USA* 2006;**103**:19093–19098.
27. Pullamsetti SS, Doebele C, Fischer A, Savai R, Kojonazarov B, Dahal BK, Ghofrani HA, Weissmann N, Grimminger F, Bonauer A, Seeger W, Zeiher AM, Dimmeler S, Schermuly RT. Inhibition of microRNA-17 improves lung and heart function in experimental pulmonary hypertension. *Am J Respir Crit Care Med* 2012;**185**:409–419.
28. Kojonazarov B, Sydykov A, Pullamsetti SS, Luitel H, Dahal BK, Kosanovic D, Tian X, Majewski M, Baumann C, Evans S, Phillips P, Fairman D, Davie N, Wayman C, Kilty I, Weissmann N, Grimminger F, Seeger W, Ghofrani HA, Schermuly RT. Effects of multikinase inhibitors on pressure overload-induced right ventricular remodeling. *Int J Cardiol* 2013;**167**:2630–2637.
29. Brittain E, Penner NL, West J, Hemnes A. Echocardiographic assessment of the right heart in mice. *J Vis Exp* 2013;**81**:e50912.
30. Dumitrascu R, Weissmann N, Ghofrani HA, Dony E, Beuerlein K, Schmidt H, Stasch JP, Gnoth MJ, Seeger W, Grimminger F, Schermuly RT. Activation of soluble guanylate cyclase reverses experimental pulmonary hypertension and vascular remodeling. *Circulation* 2006;**113**:286–295.
31. Bohlooly-Y M, Carlson L, Olsson B, Gustafsson H, Andersson IJL, Törnell J, Bergström G, Vascular function and blood pressure in GH transgenic mice. *Endocrinology* 2001;**142**:3317–3323.
32. Mulvany MJ, Halpern W. Contractile properties of small arterial resistance vessels in spontaneously hypertensive and normotensive rats. *Circ Res* 1977;**41**:19–26.
33. Katz PS, Trask AJ, Souza-Smith FM, Hutchinson KR, Galantowicz ML, Lord KC, Stewart JA, Jr., Cismowski MJ, Varner KJ, Lucchesi PA. Coronary arterioles in type 2 diabetic (db/db) mice undergo a distinct pattern of remodeling associated with decreased vessel stiffness. *Basic Res Cardiol* 2011;**106**:1123–1134.

34. Waypa GB, Chandel NS, Schumacker PT. Model for hypoxic pulmonary vasoconstriction involving mitochondrial oxygen sensing. *Circ Res* 2001;**88**:1259–1266.

35. Pak O, Sommer N, Hoeres T, Bakr A, Waisbrod S, Sydykov A, Haag D, Esfandiary A, Kojonazarov B, Veit F, Fuchs B, Weisel FC, Hecker M, Schermuly RT, Grimminger F, Ghofrani HA, Seeger W, Weissmann N. Mitochondrial hyperpolarization in pulmonary vascular remodeling. Mitochondrial uncoupling protein deficiency as disease model. *Am J Respir Cell Mol Biol* 2013;**49**:358–367.

36. Altschuld RA, Hohl CM, Castillo LC, Garleb AA, Starling RC, Brierley GP. Cyclosporin inhibits mitochondrial calcium efflux in isolated adult rat ventricular cardiomyocytes. *Am J Physiol* 1992;**262**:H1699–1704.

37. Zhao Z, Gordan R, Wen H, Fefelova N, Zang WJ, Xie LH. Modulation of intracellular calcium waves and triggered activities by mitochondrial ca flux in mouse cardiomyocytes. *PLoS One* 2013;**8**:e80574.

38. Elrod JW, Wong R, Mishra S, Vagnozzi RJ, Sakthievel B, Goonasekera SA, Karch J, Gabel S, Farber J, Force T, Brown JH, Murphy E, Molkentin JD. Cyclophilin D controls mitochondrial pore-dependent Ca(2+) exchange, metabolic flexibility, and propensity for heart failure in mice. *J Clin Invest* 2010;**120**:3680–3687.

39. Kumar S. P66Shc and vascular endothelial function. *Biosci Rep* 2019;**39**:BSR20182134.

40. McMurtry IF, Davidson AB, Reeves JT, Grover RF. Inhibition of hypoxic pulmonary vasoconstriction by calcium antagonists in isolated rat lungs. *Circ Res* 1976;**38**:99–104.

41. Shimoda LA, Sham JS, Shimoda TH, Sylvester JT. L-type Ca(2+) channels, resting [Ca(2+)](i), and ET-1-induced responses in chronically hypoxic pulmonary myocytes. *Am J Physiol Lung Cell Mol Physiol* 2000;**279**:L884–894.

42. Suresh K, Shimoda LA. Lung circulation. *Compr Physiol* 2016;**6**:897–943.

43. Robertson TP, Dipp M, Ward JP, Aaronson PI, Evans AM. Inhibition of sustained hypoxic vasoconstriction by Y-27632 in isolated intrapulmonary arteries and perfused lung of the rat. *Br J Pharmacol* 2000;**131**:5–9.

44. Drexler ES, Bischoff JE, Slifka AJ, McCowan CN, Quinn TP, Shandas R, Ivy DD, Stenmark KR. Stiffening of the extrapulmonary arteries from rats in chronic hypoxic pulmonary hypertension. *J Res Natl Inst Stand Technol* 2008;**113**:239–249.

45. Lebiedzinska M, Duszynski J, Rizzuto R, Pinton P, Wieckowski MR. Age-related changes in levels of p66Shc and serine 36-phosphorylated p66Shc in organs and mouse tissues. *Arch Biochem Biophys* 2009;**486**:73–80.

46. Liu F, Gamez G, Myers DR, Clemmons W, Lam WA, Jobe SM. Mitochondrially mediated integrin alphaIIbbeta3 protein inactivation limits thrombus growth. *J Biol Chem* 2013;**288**:30672–30681.

47. Di Lisa F, Kaludercic N, Carpi A, Menabo R, Giorgio M. Mitochondrial pathways for ROS formation and myocardial injury: the relevance of p66(Shc) and monoamine oxidase. *Basic Res Cardiol* 2009;**104**:131–139.

48. Graiani G, Lagrasta C, Migliaccio E, Spillmann F, Meloni M, Madeddu P, Quaini F, Padura IM, Lanfrancone L, Pelicci P, Emanueli C. Genetic deletion of the p66Shc adaptor protein protects from angiotensin II-induced myocardial damage. *Hypertension* 2005;**46**:433–440.

49. Bogaard HJ, Abe K, Vonk Noordegraaf A, Voelkel NF. The right ventricle under pressure: cellular and molecular mechanisms of right-heart failure in pulmonary hypertension. *Chest* 2009;**135**:794–804.

50. Zaffran S, Kelly RG, Meilhac SM, Buckingham ME, Brown NA. Right ventricular myocardium derives from the anterior heart field. *Circ Res* 2004;**95**:261–268.

Translational perspective

Pulmonary hypertension is a progressive disease of the pulmonary vasculature ultimately resulting in right heart failure. Thus, therapeutic options targeting specifically the pulmonary vasculature are urgently needed. Our study describes for the first time the role of the proteins p66shc and CypD in the regulation of the pulmonary vascular tone. As the effect of p66shc$^{-/-}$ was specific for the pulmonary vasculature, it is an interesting target for future research on therapies for pulmonary vascular diseases like pulmonary hypertension.